Science Bulletin 64 (2019) 774–781

Contents lists available at ScienceDirect

Science Bulletin

journal homepage: www.elsevier.com/locate/scib

Science Bulletin
www.scibull.com

Article

Efficient soluble deep blue electroluminescent dianthracenylphenylene emitters with CIE y ($y \leq 0.08$) based on triplet-triplet annihilation

Ling Peng [1], Jing-Wen Yao [1], Mei Wang, Lin-Ye Wang, Xiao-Lan Huang, Xin-Feng Wei, Dong-Ge Ma *, Yong Cao, Xu-Hui Zhu *

State Key Laboratory of Luminescent Materials and Devices, and Institute of Polymer Optoelectronic Materials and Devices, South China University of Technology (SCUT), Guangzhou 510640, China

ARTICLE INFO

Article history:
Received 4 March 2019
Received in revised form 31 March 2019
Accepted 18 April 2019
Available online 26 April 2019

Keywords:
Anthracene
Deep blue emission
Fluorescence
Organic light-emitting diodes
Triplet-triplet annihilation

ABSTRACT

It has been challenging to develop deep blue organic molecular fluorescent emitters with CIE y ($y \leq 0.08$) based on triplet-triplet annihilation (TTA). Here, we report facilely available dianthracenylphenylene-based emitters, which have a 3,5-di(4-*t*-butylphenyl)phenyl moiety at the one end and 4-cyanophenyl or 3-pyridyl at the other end, respectively. Both fluorophores show a high glass transition temperature of over 220 °C with a thermal decomposition temperature of over 430 °C at an initial weight loss of 1%. The preliminary characterizations of the organic light-emitting diodes (OLEDs) that utilized these nondoped emitters provided high EQEs of 4.6%–5.9% with CIE coordinates (0.15, 0.07–0.08). The analysis of the EL transient decay revealed that TTA contributed to the observed performance. The results show that the new emitters are attractive as a potential TTA-based host to afford stable deep blue fluorescent OLEDs.

1. Introduction

Organic blue-emitting fluorophores based on triplet–triplet annihilation (TTA) have received a considerable attention for organic light-emitting displays and solid-state lighting technologies [1–24]. Due to harvesting the triplet excitons, organic light-emitting diodes (OLEDs) that utilize TTA upconversion can achieve a maximal theoretical internal quantum efficiency (IQE) of 62.5% and hence an external quantum efficiency (EQE) of up to 12.5%.

Triplet-triplet annihilation was proposed in the early 1960s to account for the delayed fluorescence observed from the solutions of phenanthrene and anthracene [25] and in their molecular crystals and some other polycyclic aromatic hydrocarbons (PAHs) [26–28].

Consequently, it is conceivable that a large number of blue organic electroluminescent (EL) materials involving the TTA process have been built on PAHs. They have been explored as hosts or dopants of the emitting layers (EML) as well as nondoped emitters [1–24]. While nondoped blue TTA-based OLEDs have recently acquired EQEs of ca.9%–10% in the bottom-emission configuration with CIE y of (0.10–0.19) [13,14], the doped counterparts have provided even higher EQEs amounting to 12% with the TTA contribution, thus reaching the upper limit [12,15,19].

A donor-acceptor type dianthracenylphenylene emitter (BD3) that featured a *p*-methoxyphenyl moiety at the one end and *p*-cyanophenyl at the other hand in the simple OLEDs (ITO/TAPC/EML/B3PyPB/LiF/Al) produced a maximal EQE of 4.2% in the neat film with CIE coordinates (0.24, 0.17) [12]. By contrast, blending BD3 in the 4,4′-bis(carbazol-9-yl)biphenyl (CBP) host afforded a remarkably increased EQE of 12% at low luminance with CIE coordinates (0.15, 0.06), which showed severe efficiency roll-off possibly due to the low dopant concentration. Nevertheless, introducing a TTA-based blue-emitting host may lead to improving both the OLED efficiency and efficiency roll-off owing to the combinational effects of efficient energy transfer, reduced concentration quenching and balanced charge injection/transport in the emitting layer [5–7,17–24]. Furthermore, highly stable OLEDs that contained the TTA-based host and conventional blue fluorescent dopant have been reported with lifetime of t_{95} exceeding hundreds of hours @ 1,000 cd m^{-2} [21–24] since shortening of the exciton decay lifetime would alleviate the polaron–exciton annihilation, which represents a major degradation passway for devices harnessing triplet excitons [29–33].

It has been very demanding to develop high-performing TTA-based blue OLEDs with CIE ($y \leq 0.08$) to meet the requirements

* Corresponding authors.
E-mail addresses: msdgma@scut.edu.cn (D.-G. Ma), xuhuizhu@scut.edu.cn (X.-H. Zhu).
[1] These authors contributed equally to this work.

https://doi.org/10.1016/j.scib.2019.04.029
2095-9273/

of the NTSC standard ($y = 0.08$) and high-definition television (HDTV) ITU-R BT.709 ($y = 0.06$). Moreover, a small CIE y is beneficial to decrease the power consumption. In this context we report herein deep blue dianthracenylphenylene-based emitters **DAPBN** and **DAPPy** (Fig. 1). It has been shown that coupling the *p*-cyanophenyl moiety with the anthracenyl unit promotes the TTA upconversion [12–14]. Meanwhile, the 3,5-di(4-*t*-butylphenyl) phenyl moiety is utilized to suppress strong intermolecular interactions, tune the emission color and increase the solubility for facilitating purification [34,35]. Both emitters combine the advantages of high EQEs of 4.6%−5.9% with low efficiency roll-off and deep blue emission with the respective CIE coordinates (0.15, 0.08) and (0.15, 0.07) and high glass transition temperatures (T_g) of over 220 °C.

2. Experimental

2.1. Materials and instructions

All manipulations involving air-sensitive reagents were performed under an inert of dry nitrogen. 9-Bromo-10-(3,5-bis(4-*t*-butylphenyl)phenyl)anthracene (**1**) [34,35] and 4-(10-bromoan thracen-9-yl)benzonitrile (**6**) [12] were reported in literature. All the other starting materials were purchased commercially and used as received, unless otherwise specified.

^{1}H NMR measurements were carried out on Bruker 400 and 500 MHz DRX spectrometers with tetramethylsilane (TMS) as the internal reference. Mass spectroscopy was obtained on a Waters ACQUITY TQD liquid chromatograph-mass spectrometer using APCI ionization. Thermogravimetric analysis measurements were carried out on Netzsch TG 209 under a nitrogen flow at a heating rate of 20 °C min^{-1}. Differential scanning calorimetry measurements were performed on a Netzsch DSC 204 under nitrogen at a heating and cooling rate of 10 and 20 °C min^{-1} respectively. UV-Vis absorption spectra were recorded on an HP 8453 UV-Vis spectrophotometer. PL spectra were recorded on an HORIBA Fluorolog-3 fluorescence spectrophotometer. PL quantum yields (PLQYs) of the nondoped films were measured utilizing an integrating sphere of Hamamatsu absolute PL quantum yield spectrometer (C9920-02G). Transient PL decay were evaluated with 340 nm LED excitation source for the nondoped film.

2.1.1. 9-(4-bromophenyl)-10-(3,5-bis(4-t-butylphenyl)phenyl) anthracene (*2*)

$Pd(PPh_3)_4$ (120 mg, 0.10 mmol) was added quickly to a mixture of 9-bromo-10-(3,5-bis(4-*t*-butylphenyl)phenyl)anthracene (5 g, 8.3 mmol), 4-bromophenylboronic acid (2 g, 10 mmol) and K_2CO_3 aqueous solution (2 mol L^{-1}, 10 mL) in toluene (50 mL) and ethanol (6 mL) under N_2. The reaction was heated at 90 °C for 12 h. After being cooled to room temperature, the crude product was concentrated and distilled water was added. The organic layer was separated, dried over anhydrous $MgSO_4$, filtered and concentrated under reduced pressure. The residue was purified by column chromatography using petroleum ether as eluent to afford a yellowish solid. Yield: 2.5 g (44%). ^{1}H NMR (400 MHz, $CDCl_3$) δ 8.03 (s, 1H), 7.87–7.85 (m, 2H), 7.76–7.74 (m, 2H), 7.69–7.66 (m, 8H), 7.50–7.48 (m, 4H), 7.39–7.34 (m, 6H), 1.37 (s, 18H). ^{13}C NMR (126 MHz, $CDCl_3$) δ 150.73, 141.55, 139.21, 137.76, 137.71, 131.04, 130.26, 128.48, 127.84, 127.53, 126.99, 126.90, 125.85, 125.66, 124.91, 122.81, 34.56, 31.34.

2.1.2. 2-(4-(10-(3,5-bis(4-t-butylphenyl)phenyl)anthracen-9-yl) phenyl)-4,4,5,5-tetramethyl-1,3,2-dioxaborolane (*3*)

$Pd(PPh_3)_2Cl_2$ (105 mg, 0.15 mmol) was added to a mixture of compound **2** (2 g, 3 mmol), bis(pinacolato)diboron (1.2 g, 4.5 mmol) and aqueous KOAc (900 mg, 9 mmol) in THF (50 mL) under N_2. The reaction was heated at 80 °C overnight. After being cooled to room temperature, the crude product was concentrated and distilled water was added. The organic layer was extracted with CH_2Cl_2, separated, dried over anhydrous $MgSO_4$, filtered and concentrated under reduced pressure. The residue was subjected to column chromatography over silica gel using petroleum ether/CH_2Cl_2 as eluent to afford a yellowish solid. Yield: 2 g (93%). ^{1}H NMR (400 MHz, $CDCl_3$) δ 8.08–8.06 (m, 2H), 8.03–8.02 (m, 1H), 7.87–7.84 (m, 2H), 7.70–7.68 (m, 8H), 7.54–7.52 (m, 2H), 7.49 (d, J = 8.32 Hz, 4H), 7.35–7.30 (m, 4H), 1.43 (s, 12H), 1.37 (s, 18H). ^{13}C NMR (126 MHz, $CDCl_3$) δ 150.61, 142.2, 141.46, 139.86, 137.95, 137.11, 137.06, 134.80, 130.82, 129.86, 129.71, 128.71, 127.10, 126.91, 125.83, 125.14, 125.10, 124.67, 83.95, 34.57, 31.36, 24.97.

2.1.3. 4-(10-bromoanthracen-9-yl)benzonitrile (*6*)

N-Bromosuccinimide (NBS) (3.5 g, 19.5 mmol) was added in three portions at 50 °C to compound **5** (3.5 g, 19.5 mmol) in CH_2Cl_2 (30 mL) in the absence of light. The completion of bromination was confirmed by TLC. The crude product was washed with ethanol to afford a golden solid. Yield: 6.3 g (90%). ^{1}H NMR (500 MHz, $CDCl_3$) δ 8.63 (d, J = 8.9 Hz, 2H), 7.90–7.88 (m, 2H), 7.62–7.59 (m, 2H), 7.54–7.52 (m, 2H), 7.48 (d, J = 8.7 Hz, 2H), 7.42–7.39 (m, 2H). ^{13}C NMR (126 MHz, $CDCl_3$) δ 143.71, 143.68, 135.09, 132.31, 132.06, 130.39, 130.12, 128.12, 127.12, 126.41, 126.26, 123.93, 118.74, 111.91.

2.1.4. 3-(anthracen-9-yl)pyridine (*8*)

$Pd(PPh_3)_4$ (120 mg, 0.10 mmol) was added quickly to a mixture of 3-(4,4,5,5-tetramethyl-1,3,2-dioxaborolan-2-yl)pyridine (5 g, 24 mmol), 9-bromoanthracene (7.4 g, 28.8 mmol) and K_2CO_3 aqueous solution (2 mol L^{-1}, 30 mL) in toluene (100 mL) and ethanol

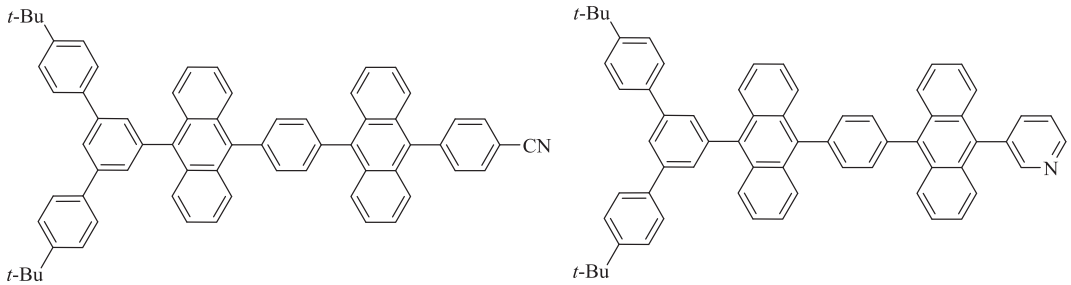

Fig. 1. Chemical structures of (a) **DAPBN**, (b) **DAPPy**.

(15 mL) under N_2. The reaction was heated at 90 °C for 12 h. After being cooled to room temperature, the crude product was concentrated and distilled water was added. The organic layer was separated, dried over anhydrous $MgSO_4$, filtered and concentrated under reduced pressure. The crude product was purified with column chromatography using petroleum ether/CH_2Cl_2 as eluent and further washed with ethanol to afford to afford a white solid in 51% yield (3.1 g). ^{1}H NMR (400 MHz, $CDCl_3$) δ 8.804 (dd, J = 4.9, 1.5 Hz, 1H), 8.70 (d, J = 1.6 Hz, 1H), 8.55 (s, 1H), 8.07 (d, J = 8.5 Hz, 2H), 7.81–7.74 (m, 1H), 7.59–7.53 (m, 3H), 7.52–7.44 (m, 2H), 7.40–7.36 (m, 2H). ^{13}C NMR (126 MHz, $CDCl_3$) δ 151.72, 148.86, 138.85, 134.63, 132.53, 131.26, 130.43, 128.54, 127.57, 126.02, 125.96, 125.27, 123.37.

2.1.5. 3-(10-bromoanthracen-9-yl)pyridine (**9**)

This compound was synthesized by a method similar to that for compound **6**. The crude product was purified with column chromatography using petroleum ether/CH_2Cl_2 as eluent and further washed with ethanol to afford to afford a white solid in 95% yield. ^{1}H NMR (400 MHz, $CDCl_3$) δ 8.83 (s, 1H), 8.68 (s, 1H), 8.64 (d, J = 8.9 Hz, 2H), 7.79–7.77 (m, 1H), 7.63–7.54 (m, 5H), 7.44–7.40 (m, 2H). ^{13}C NMR (126 MHz, $CDCl_3$) δ 151.53, 149.16, 138.71, 134.29, 133.27, 131.17, 130.18, 128.10, 127.08, 126.58, 126.17, 123.91, 123.40.

2.1.6. 4-(10-(4-(10-(3,5-bis(4-t-butylphenyl)phenyl)anthracen-9-yl) phenyl)anthracen-9-yl)- benzonitrile (***DAPBN***)

$Pd(PPh_3)_4$ (32 mg, 0.028 mmol) was added quickly to a mixture of compound **3** (1 g, 1.4 mmol), compound **6** (0.5 g, 1.4 mmol) and K_2CO_3 aqueous solution (2 mol L^{-1}, 2 mL) in toluene (40 mL) and ethanol (2 mL) under N_2. The reaction was stirred at 90 °C for 12 h. After being cooled to room temperature, the crude product was concentrated and distilled water was added. The organic layer was separated, dried over anhydrous $MgSO_4$, filtered and concentrated under reduced pressure. The residue was purified by column chromatography using petroleum ether/CH_2Cl_2 as eluent and further washed with n-hexane to afford a yellowish solid. Yield: 1.1 g (91%). ^{1}H NMR (500 MHz, $CDCl_3$) δ 8.06 (m, 1H), 8.02–7.93 (m, 8H), 7.77– 7.67 (m, 12H), 7.61 (d, J = 8.75 Hz, 2H), 7.53–7.48 (m, 8H), 7.46–7.40 (m, 4H), 1.38 (s, 18H). ^{13}C NMR (126 MHz, $CDCl_3$) δ 150.66, 144.56, 141.54, 139.84, 138.53, 138.05, 137.95, 137.83, 137.36, 136.78, 134.71, 132.35, 132.33, 131.52, 131.31, 130.05, 130.03, 129.95, 129.51, 128.74, 127.31, 126.94, 126.16, 125.85, 125.46, 125.36, 125.27, 124.76, 118.92, 111.67, 34.58, 31.37. MS (APCI) m/z: [M+H$^+$]: calcd. for $C_{67}H_{53}N$, 872.42; Found, 872.9 (100%). Anal. calcd. For $C_{67}H_{53}N$: C 92.27, H 6.13, N 1.61. Found: C 92.24, H 6.37, N 1.55.

2.1.7. 3-(10-(4-(10-(3,5-bis(4-t-butylphenyl)phenyl)anthracen-9-yl) phenyl)anthracen-9-yl) pyridine (***DAPPy***)

This compound was synthesized by a method similar to that for compound **DAPBN**, using compound **9** and compound **6** instead. The crude product was purified by column chromatography using petroleum ether/CH_2Cl_2 as eluent and further washed with n-hexane to afford to afford a yellowish solid in 95% yield. ^{1}H NMR (400 MHz, $CDCl_3$) δ 8.876 (dd, J = 4.8, 1.1 Hz, 1H), 8.827 (d, J = 1.24 Hz, 1H), 8.09–7.93 (m, 8H), 7.77–7.65 (m, 13H), 7.55–7.41 (m, 12H), 1.38 (s, 18H). ^{13}C NMR (126 MHz, $CDCl_3$) δ 151.70, 150.67, 148.78, 141.54, 139.87, 139.18, 138.49, 138.02, 137.97, 137.96, 137.93, 137.33, 136.84, 135.08, 132.72, 131.54, 131.50, 131.37, 131.30, 130.28, 130.06, 130.03, 130.01, 128.76, 127.30, 126.95, 126.31, 125.86, 125.80, 125.45, 126.36, 126.28, 124.75, 123.55, 34.59, 31.37. MS (APCI) m/z: [M+H$^+$]: calcd. for $C_{65}H_{53}N$, 848.41; Found, 848.6 (100%). Anal. calcd. For $C_{65}H_{53}N$: C 92.05, H 6.30, N 1.65. Found: C 91.72, H 6.33, N 1.59.

2.2. OLED fabrication and characterizations

DAPBN and **DAPPy** were evaluated as the nondoped emitters in OLEDs (ITO/HATCN(15 nm)/TAPC(60 nm)/TCTA(10 nm)/Emitter (20 nm)/TPBi(40 nm)/LiF(1 nm)/Al). The OLEDs were fabricated by evaporating each layer onto ITO substrate sequentially at pressures of ca. 4×10^{-6} Pa. Before transferring to a deposition chamber, the ITO substrates were cleaned by ultra-sonication in detergents and deionized water, dried in an oven at 120 °C for 1 h, and finally subjected to oxygen plasma treatment for 6 min. Then, the vacuum evaporation rates of organic materials were deposited at (0.1–0.15) nm s^{-1}. Finally, a 1-nm-thick layer of LiF was deposited at 0.02 nm s^{-1} and the metallic cathode (Al) of 120 nm thick was deposited at a rate of 0.5–0.8 nm s^{-1}. The effective emission area of the devices is (4×4) mm^2. All the OLEDs were measured without encapsulation at room temperature in the ambient. The Current density–Voltage–Luminance (*J-V-L*) characteristics were measured with a Keithley 2400 source meter and a LS110 luminance meter. The electroluminescence (EL) spectra were collected using a spectrascan PR650 spectrophotometer. The EQEs were calculated from the Luminance-Current density characteristics and EL spectra with the hypothesis of Lambertian distribution. The transient EL decay was tested by an Agilent 8114A pulse generator to generate rectangular pulse voltages.

3. Results and discussion

3.1. Synthesis

The synthesis of compounds **DAPBN** and **DAPPy** is straightforward and outlined in Fig. 2, involving the Suzuki coupling of 4-(10-bromoanthracen-9-yl)benzonitrile (**6**) [12] and 3-(10-bromoanthracen-9-yl)pyridine (**9**) with the 3,5-bis(4-*t*-butylphenyl)phenyl-tethered (anthracen-9-yl)phenylboron ester (**3**) [12,34,35] in ca. 90% yield, respectively. Compound **9** was facilely obtained successively through Suzuki reaction of 9-bromoanthracene with 3-(4,4,5,5-tetramethyl-1,3,2-dioxaboro lan-2-yl)pyridine (**7**) and subsequently selective bromination.

The identity and purity of the new emitters **DAPBN** and **DAPPy** are confirmed by ^{1}H NMR, mass spectroscopy and elemental analysis (Figs. S1–S3 online). By introducing the 3,5-bis(4-*t*-butylphenyl)phenyl moiety, **DAPBN** and **DAPPy** exhibit good solubility in weakly polar organic solvents, for instance, over 20 mg mL^{-1} in toluene, which facilitates purification.

3.2. Photophysical properties

The absorption spectra of **DAPBN** and **DAPPy** exhibited similar absorption profiles in the range of 340–400 nm both in dilute toluene solution and as neat films (Fig. 3 and Table 1), which are attributed to the vibrational structure of the anthracene unit. Note that the major spectral shift is very small by ca. 2 nm from solution to the solid state. The optical bandgap for both compounds were estimated as 2.91 eV, based on the absorption onset of the films.

We then studied the photoluminescence (PL) of **DAPBN** and **DAPPy** in different solvents (Fig. S4 and Table S1 online). It showed that even the strongly polar solvent DMF failed to produce substantial changes on the emission spectra with respect to non-polar *n*-hexane, indicating that intramolecular charge transfer is not significant in particular with **DAPPy**. Specifically, the emission peak of **DAPPy** was shifted only by 6 vs. 12 nm for **DAPBN** when replacing n-hexane by DMF, presumably due to the robust electron-withdrawing ability of the cyano moiety. In addition, films of **DAPBN** and **DAPPy** exhibited bright deep blue fluorescence respectively at 447 and 440 nm with a narrow full width at half

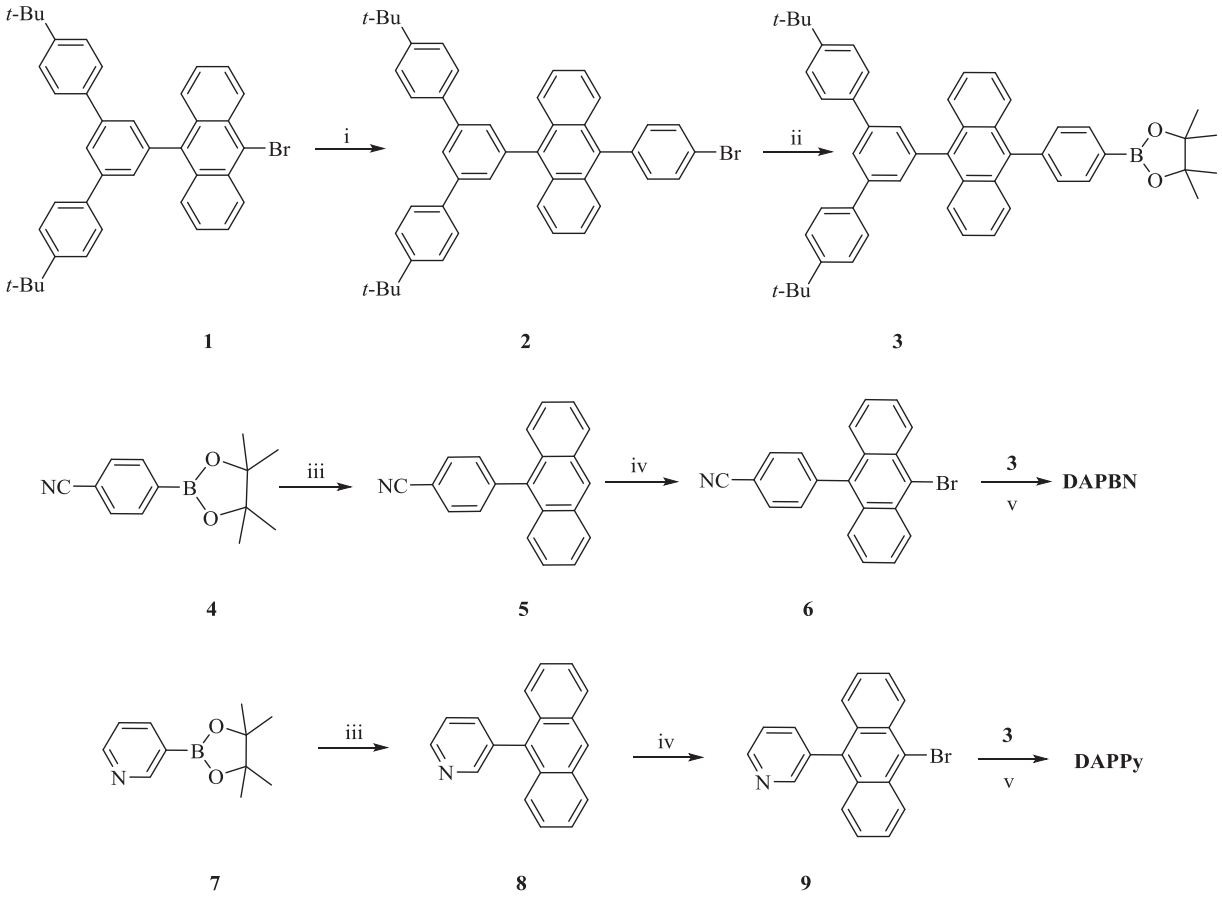

Fig. 2. Synthetic routes to DAPBN and DAPPy: (i) 4-bromophenylboronic acid, $Pd(PPh_3)_4$, 2 mol L^{-1} K_2CO_3 aqueous solution, ethanol, toluene, 90 °C; (ii) bis(pinacolato) diboron, $Pd(PPh_3)_2Cl_2$, anhydrous KOAc, THF, 80 °C; (iii) 9-bromoanthracene, $Pd(PPh_3)_4$, 2 mol L^{-1} K_2CO_3 aqueous solution, ethanol, toluene, 90 °C; (iv) NBS, CH_2Cl_2, 50 °C; (v) $Pd(PPh_3)_4$, 2 mol L^{-1} K_2CO_3 aqueous solution, ethanol, toluene, 90 °C.

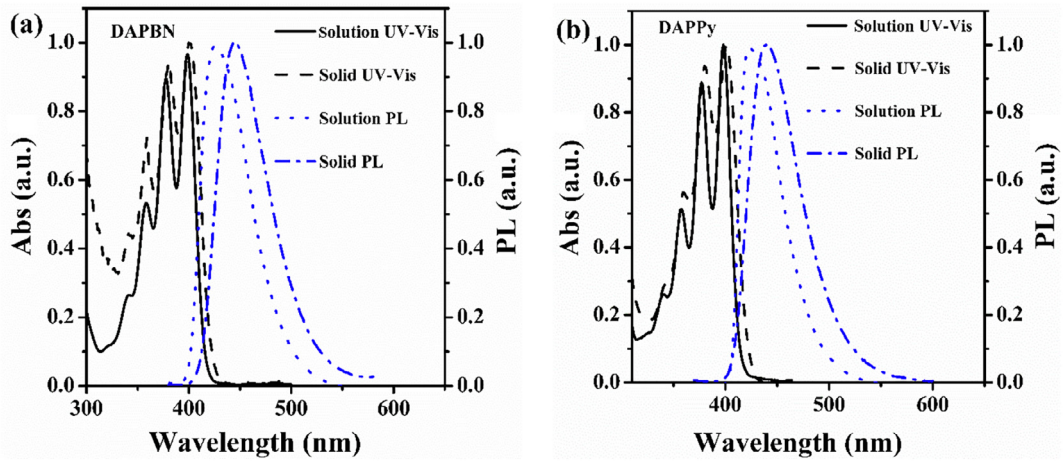

Fig. 3. (Color online) Normalized UV-Vis and fluorescence spectra of (a) **DAPBN** and (b) **DAPPy** in dilute toluene solutions (1.0×10^{-5} mol L^{-1}) and as films on quartz (ca. 45 nm), spin-cast from a toluene solution (10 mg mL^{-1}). The fluorescence spectra were recorded under excitation wavelength of 340 nm.

maxima (FWHM) of 50–60 nm, yielding a redshift of 22 and 17 nm from toluene solution (Fig. 3 and Table 1).

The absolute solid photoluminescence quantum yields (PLQYs) were measured in an integrating sphere as 35.2% for **DAPBN** and 16.0% for **DAPPy**. Therefore, the PLQY of **DAPBN** appeared comparable to that of the donor-acceptor dianthracenylphenylene compound BD3 and nevertheless greatly improved relative to 1,4-bis (10-phenylanthracene-9-yl)benzene and 1-(10-phenylanthracen-9-yl)-4-(10-(4-cyanophenyl)anthracen-9-yl)benzene, revealing that the 3,5-di(4-*t*-butylphenyl)phenyl endgroup could effectively reduce the concentration quenching [12].

3.3. Thermal properties

Thermal gravimetric analysis (TGA) showed that **DAPBN** and **DAPPy** began to decompose at ca. 437 and 451 °C with an initial

Table 1
Optical and electrochemical data of **DAPBN** and **DAPPy**.

	UV-Vis (λ_{max}, nm)		E_g (eV)	PL (λ_{max}, nm)		PLQY (%)[c]	E_{ox} (V)[d]	HOMO/LUMO (eV)[e]
	Solution[a]	Solid[b]		Solution[a]	Solid (FWHM)[b]			
DAPBN	341, 358, 377, 398	341, 360, 381, 400	2.91	425	447(58)	35.2	1.07	−5.53/−2.62
DAPPy	339, 356, 376, 398	341, 360, 381, 400	2.91	423	440(57)	16	1.08	−5.54/−2.63

[a] In toluene (~10^{-5} mol L^{-1}).
[b] As films spin-cast on quartz from toluene solution of 10 mg mL^{-1}.
[c] PL quantum yields (PLQYs) measured in an integrating sphere under 320 nm laser excitation as films on quartz from the toluene solution of 20 mg mL^{-1}.
[d] Measured from the onset value of the oxidation potential vs. Ag/AgCl reference electrode.
[e] HOMO derived from the onset E_{ox} values with reference to the energy level of ferrocene of − 4.8 eV vs. vacuum level. LUMO calculated from the HOMO and the optical band gap E_g.

weight loss of about 1% (Fig. S5 online), respectively. Differential scanning calorimetry (DSC) measurements revealed high glass transition temperatures (T_g) of 234 °C for **DAPBN** and 227 °C for **DAPPy** (Fig. 4). **DAPBN** melted at 349 °C in the first heating. However, no melting was observed by introducing the 3-pyridyl moiety instead even heated up to 450 °C.

3.4. Electrochemical properties

The electrochemical properties of the new compounds are characterized by cyclic voltammetry performed in CH_2Cl_2 in the presence of n-Bu_4NPF_6 (0.1 mol L^{-1}) as supporting electrolyte. **DAPBN** and **DAPPy** displayed a quasi-reversible oxidation with the onset at 1.07 and 1.08 V vs. Ag/AgCl, respectively (Fig. S6 online). Based on the electrochemical data, the HOMO levels were estimated as −5.53 eV for **DAPBN** and −5.54 eV for **DAPPy** with reference to the energy level of ferrocene. Therefore, the LUMO levels for the two compounds were similar as −2.62 and −2.63 eV, roughly derived from the corresponding HOMO level and absorption onset of their thin films.

3.5. Carrier transport properties

In order to understand the charge transport properties of the new emitters, the electron-only devices (EOD) (ITO/LiF(1 nm)/TPBi (10 nm)/Emitter(100 nm)/TPBi(10 nm)/LiF(1 nm)/Al) and hole-only devices (HOD) (ITO/HATCN(5 nm)/TAPC(10 nm)/Emitter (100 nm)/TAPC(10 nm)/HATCN(5 nm)/Al) devices were fabricated (Fig. 5). TPBi = 1,3,5-tris(*N*-phenyl-benzimidazolyl)benzene, HATCN = dipyrazino[2,3-f:2′,3′-h]quinoxaline-2,3,6,7,10,11-*hexa*-carbonitrile and TAPC = 1,1-bis((di-4-tolylamino)phenyl)cyclohexane.

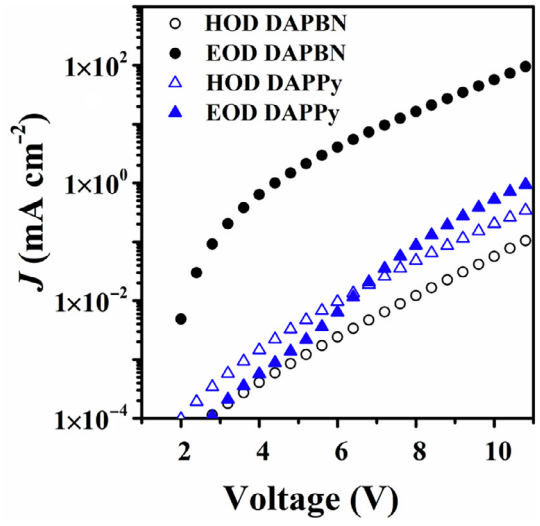

Fig. 5. (Color online) Current density-voltage (*J-V*) characteristics of the electron-only devices (ITO/LiF(1 nm)/TPBi(10 nm)/Emitter(100 nm)/TPBi(10 nm)/LiF(1 nm)/Al) and hole-only devices (ITO/HATCN(5 nm)/TAPC(10 nm)/Emitter(100 nm)/TAPC (10 nm)/HATCN(5 nm)/Al). Emitter = **DAPBN** or **DAPPy**.

The Current density-Voltage (*J-V*) characteristics of the single-carrier devices plotted in a logarithm scale ($\ln(J/E^2)$ vs. $E^{1/2}$) exhibited a space-charge-limited current (SCLC) behavior at ca. (2–5) × 10^5 V cm^{-1} and can be described by the equation of SCLC with field-dependent mobility (Fig. S7 and Table S2 online) [36].

After fitting the $\ln(J/E^2)$–$E^{1/2}$ curves, **DAPPy** appeared to exhibit a higher hole mobility with (8×10^{-9}–5.3×10^{-8}) cm^2 V^{-1} s^{-1} at

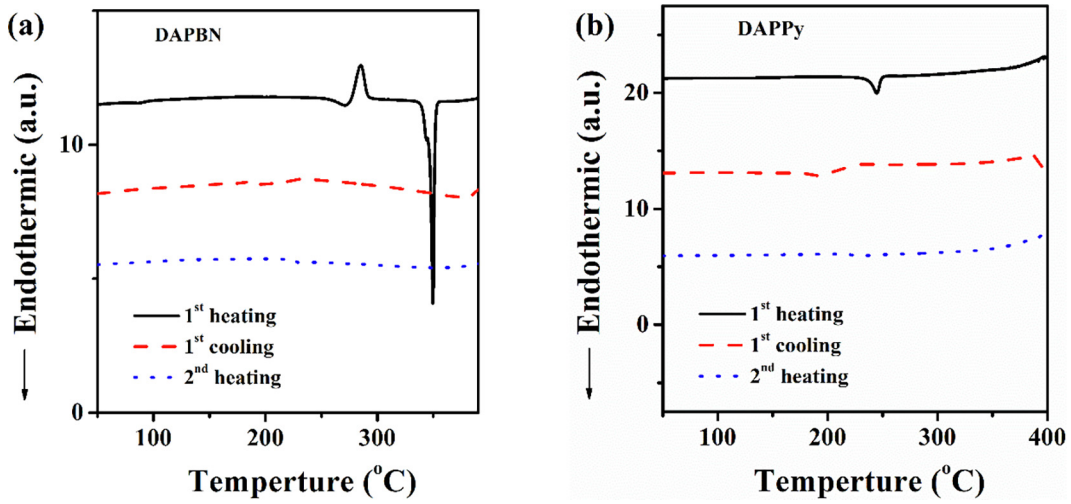

Fig. 4. (Color online) DSC diagrams of (a) **DAPBN** and (b) **DAPPy**.

$E = (2–5) \times 10^5$ V cm^{-1} vs. $(3.1 \times 10^{-9}–1.4 \times 10^{-8})$ cm^2 V^{-1} s^{-1} for **DAPBN**. However, **DAPBN** showed orders of magnitude higher electron mobility of $(3.6 \times 10^{-6}–2.3 \times 10^{-5})$ cm^2 V^{-1} s^{-1} at $E = (2–5) \times 10^5$ V cm^{-1} vs. $(1.8 \times 10^{-9}–2.6 \times 10^{-8})$ cm^2 V^{-1} s^{-1} for **DAPPy**.

3.6. Electroluminescent properties

DAPBN and **DAPPy** were first characterized as the nondoped emitters in OLEDs (ITO/HATCN(15 nm)/TAPC(60 nm)/TCTA (10 nm)/Emitter(20 nm)/TPBi(40 nm)/LiF(1 nm)/Al). TCTA = 4,4′,4″-tris(*N*-carbazolyl)triphenylamine. All the layers excluding ITO were deposited by thermal sublimation. The chemical structures as well as the HOMO/LUMO levels of organic materials involved in the devices are shown in Fig. S8 (online).

Both the nondoped OLEDs exhibited deep blue EL emission with CIE coordinates of (0.15, 0.08) and (0.15, 0.07), respectively (Fig. 6 and Table 2). The EL spectra peaking at ~450 nm closely resembled the corresponding PL emission in the solid films, indicating that the exciton recombination was confined in the emitting layer and that no exciplex emission occurred with the adjacent charge-transport materials. Moreover, the deep blue OLEDs possessed remarkable color stability with practically no variation of the EL spectra over a wide range of driving voltages (Fig. S9 online).

It is interesting to note that initially **DAPBN** and **DAPPy** based OLEDs showed an enhanced current efficiency (*CE*) with increasing the luminance, since more triplet excitons would be fused into singlets through TTA upconversion with increasing the current density. As a result, the devices achieved a maximal *CE* of 4.46 cd A^{-1} @ ca. 1,298 cd m^{-2} (corresponding to 5.97% EQE) and 3.11 cd A^{-1} @ ca. 813 cd m^{-2} (4.61% EQE), respectively (Figs. 6a, b and S10 online). With respect to **DAPPy**, the **DAPBN** OLED displayed a very small efficiency roll-off. Even at a luminance of ca. 4,300 cd m^{-2}, *CE* remained as high as 4.0 cd A^{-1} (5.35% EQE), which could be attributed to its higher PLQY and electron mobility and further harnessing triplet excitons through triplet-triplet annihilation discussed below.

It is well-known that anthracene-based luminophores are prone to undergo triplet-triplet annihilation upconversion [1–4,20,25–28,37]. The nonlinear Luminance–Current density characteristics of the nondoped deep blue OLEDs at low current density (Fig. S11 online) supported that TTA participated in the fluorescence processes of the new compounds **DAPBN** and **DAPPy** [20,38].

Further we measured the transient EL decay of both OLEDs at different driving voltages (Figs. 7 and S12 online). A delayed EL component in the time range of microseconds was evidenced after the prompt decay, which was nevertheless absent in the transient

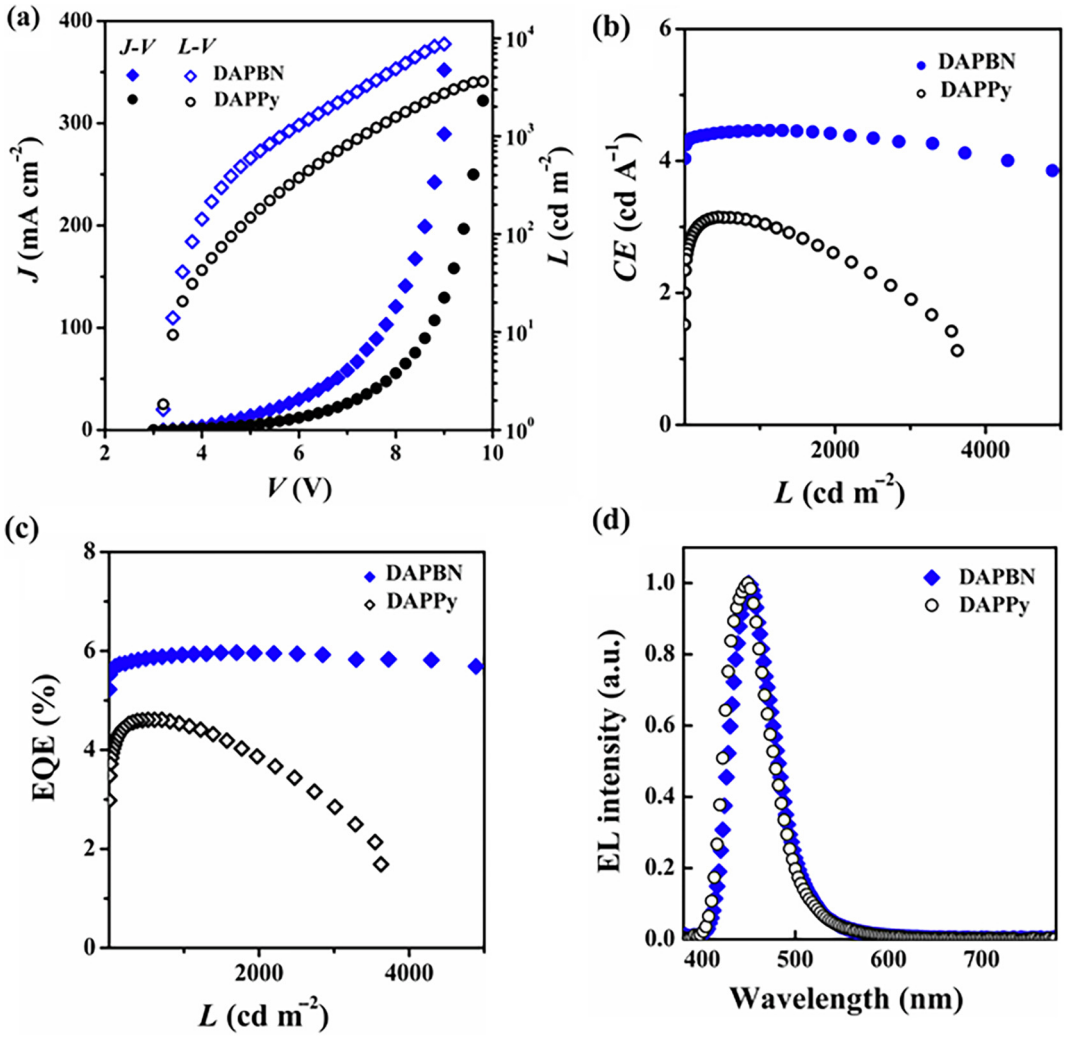

Fig. 6. (Color online) The EL characteristics of the deep blue nondoped OLEDs (ITO/HATCN/TAPC/TCTA/**DAPBN** or **DAPPy**/TPBi/LiF/Al). (a) Current density-Voltage-Luminance (*J-V-L*), (b) Current efficiency-Luminance (*CE-L*), (c) EQE-Luminance (*EQE-L*) and (d) EL spectra.

Table 2
Summary of the EL characteristics of the deep blue nondoped OLEDs.

Emitter	FWHM (nm)	V_{on}[a] (V)	Maximum/1,000 cd m^{-2}		CIE (x, y)	EL peak (nm)
			CE (cd A^{-1})	EQE (%)		
DAPBN	54	3.2	4.46/4.46	5.97/5.94	(0.15, 0.08)	451
DAPPy	55	3.2	3.15/3.00	4.61/4.48	(0.15, 0.07)	449

[a] Defined at a luminance of ca. (1–3) cd m^{-2}.

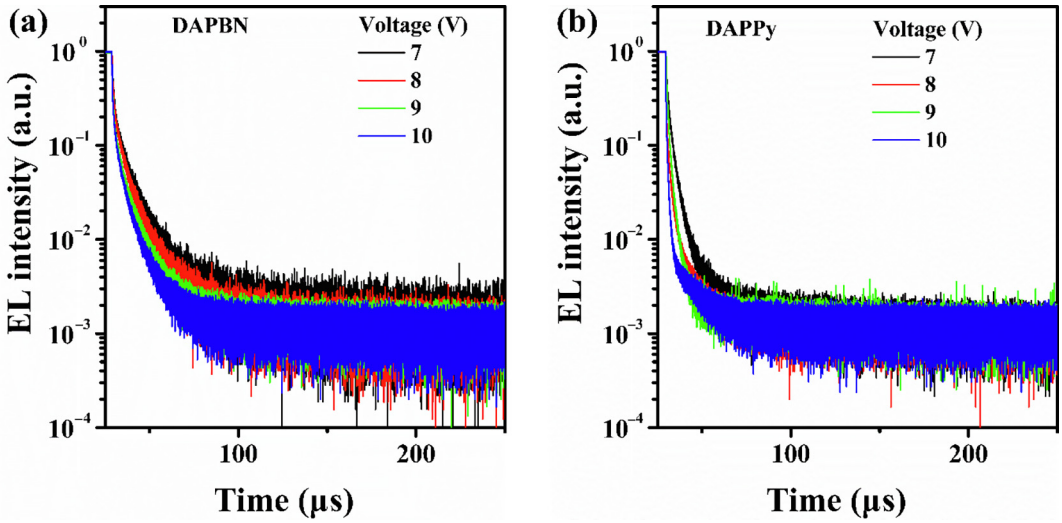

Fig. 7. The transient EL decay of the nondoped deep blue OLEDs (ITO/HATCN/TAPC/TCTA/Emitter/TPBi/LiF/Al) at different driving voltages: (a) **DAPBN**, (b) **DAPPy**.

PL performed in the ambient at room temperature (Fig. S13 online). Note that **DAPBN and DAPPy** showed the lifetime of the excited state with ca. 1.29 and 1.22 ns in the nondoped solid films, respectively. Increasing the voltage led to decreasing the delayed component due to the enhanced polaron-triplet exciton annihilation, which seemed more severe in the **DAPPy** OLED.

The logarithm of the transient EL intensity vs. time at an applied voltage of 7 V was fitted to probe the delayed component characteristics (Fig. S12 online). In both cases, the decay followed slope of ca. −1 in the initial time region and subsequently slope of ca. −2, as observed in conjugated polymers MEH-PPV and polyfluorene [39,40] and small-molecule NPB:TPBi exciplex [41] and anthracene-based emitters [13,14]. The presence of the decay at slope of ca. −2 certainly originated from TTA [39–41] while the counterpart at slope of ca. −1 was attributed to the effect of the dispersive migration of the triplet population [40].

4. Conclusions

We have reported soluble efficient deep blue dianthracenylphenylene-based molecular fluorophores, which show high thermal stability and glass transition temperatures of over 220 °C. The initial characterization of the new emitters in the nondoped OLEDs yielded high EQEs of 4.6%–5.9% with CIE y ($y \leq 0.08$), closely matching the NTSC standard. Replacing the 3-pyridyl endgroup with 4-cyanopheyl increases the PLQY and electron mobility, hence leading to improving the EQE with very small efficiency roll-off. The analysis of the transient EL decay of the nondoped deep blue OLEDs as well as the Luminance–Current density characteristics supports that triplet-triplet annihilation upconversion contributes to the fluorescent processes. The new emitters reported here shall deserve further efforts to afford stable deep blue OLEDs. Work along the line is in progress in our laboratory and will be reported in due course.

Conflict of interest

The authors declare that they have no conflict of interest.

Acknowledgments

This work was supported by the National Key R&D Program of China (2016YFB0400701), NSFC-Guangdong Joint Program (U1801258 and U1301243), Department of Science and Technology of Guangdong Province (2017A050503002) and Foundation of Guangzhou Science and Technology Project (201504010012). XHZ greatly acknowledges the support of Dongguan Major Special Project (2017215117010).

Author contributions

LP, MW, LYW and XFW contributed to the synthesis and characterization. DGM and JWY contributed to device fabrication and characterization. LP and XHZ wrote the manuscript. XHZ, DGM and YC initiated the project. XHZ conceived the idea and organized the manuscript. All the authors including XLH contributed to discussion.

Appendix A. Supplementary data

Supplementary data to this article can be found online at https://doi.org/10.1016/j.scib.2019.04.029.

References

[1] Kondakov DY. Triplet–triplet annihilation in highly efficient fluorescent organic light-emitting diodes: current state and future outlook. Philos Trans R Soc A Math Phys Eng Sci 2015;373:20140321.

[2] Chen WC, Lee CS, Tong QX. Blue-emitting organic electrofluorescence materials: progress and prospective. J Mater Chem C 2015;3:10957.
[3] Luo YJ, Lu ZY, Huang Y. Triplet fusion delayed fluorescence materials for OLEDs. Chin Chem Lett 2016;27:1223.
[4] Im Y, Byun SY, Kim JH, et al. Recent progress in high-efficiency blue-light-emitting materials for organic light-emitting diodes. Adv Funct Mater 2017;27:1603007.
[5] Li YQ, Fung MK, Xie Z, et al. An efficient pure blue organic light-emitting device with low driving voltages. Adv Mater 2002;14:1317.
[6] Shi JM, Tang CW. Anthracene derivatives for stable blue-emitting organic electroluminescence devices. Appl Phys Lett 2002;80:3201.
[7] Lee MT, Chen HH, Liao CH, et al. Stable styrylamine-doped blue organic electroluminescent device based on 2-methyl-9,10-di(2-naphthyl)anthracene. Appl Phys Lett 2004;85:3301.
[8] Lyu YY, Kwak J, Kwon O, et al. Silicon-cored anthracene derivatives as host materials for highly efficient blue organic light-emitting devices. Adv Mater 2008;20:2720.
[9] Kim SK, Yang B, Ma YG, et al. Exceedingly efficient deep-blue electroluminescence from new anthracenes obtained using rational molecular design. J Mater Chem 2008;18:3376.
[10] Cho I, Kim SH, Kim JH, et al. Highly efficient and stable deep-blue emitting anthracene-derived molecular glass for versatile types of nondoped OLED applications. J Mater Chem 2012;22:123.
[11] Kim B, Park Y, Lee J, et al. Synthesis and electroluminescence properties of highly efficient blue fluorescence emitters using dual core chromophores. J Mater Chem C 2013;1:432.
[12] Hu JY, Pu YJ, Satoh F, et al. Bisanthracene-based donor–acceptor-type light-emitting dopants: highly efficient deep-blue emission in organic light-emitting devices. Adv Funct Mater 2014;24:2064.
[13] Tang X, Bai Q, Shan T, et al. Efficient nondoped blue fluorescent organic light emitting diodes (OLEDs) with a high external quantum efficiency of 9.4% @ 1,000 cd m^{-2} based on phenanthroimidazole–anthracene derivative. Adv Funct Mater 2018;28:17058.
[14] Liu W, Ying SA, Guo RD, et al. Nondoped blue fluorescent organic light-emitting diodes based on benzonitrile-anthracene derivative with 10.06% external quantum efficiency and low efficiency roll-off. J Mater Chem C 2019;7:1014.
[15] Chen YH, Lin CC, Huang MJ, et al. Superior upconversion fluorescence dopants for highly efficient deep-blue electroluminescent devices. Chem Sci 2016;7:4044.
[16] Chou PY, Chou HH, Chen YH, et al. Efficient delayed fluorescence via triplet–triplet annihilation for deep-blue electroluminescence. Chem Commun 2014;50:6869.
[17] Pu YJ, Nakata G, Satoh F, et al. Optimizing the charge balance of fluorescent organic light-emitting devices to achieve high external quantum efficiency beyond the conventional upper limit. Adv Mater 2012;24:1765.
[18] Fukagawa H, Shimizu T, Ohbe N, et al. Anthracene derivatives as efficient emitting hosts for blue organic light-emitting diodes utilizing triplet–triplet annihilation. Org Electron 2012;13:1197.
[19] Cha SJ, Han NS, Song JK, et al. Efficient deep blue fluorescent emitter showing high external quantum efficiency. Dyes Pigm 2015;120:200.
[20] Kondakova DY. Characterization of triplet-triplet annihilation in organic light-emitting diodes based on anthracene derivatives. J Appl Phys 2007;102:114504.
[21] Lin MF, Wang L, Wong WK, et al. Highly efficient and stable sky blue organic light-emitting devices. Appl Phys Lett 2006;89:121913.
[22] Suzuki T, Nonaka Y, Watabe T, et al. Highly efficient long-life blue fluorescent organic light-emitting diode exhibiting triplet–triplet annihilation effects enhanced by a novel hole-transporting material. Jpn J Appl Phys 2014;53:052102.
[23] Chen NN, Tan WY, Liu JZ, et al. Triarylphosphine oxide–phenanthroline molecular conjugate as a promising doped electron-transport layer for organic light-emitting diodes. Org Electron 2017;48:271.
[24] Jung H, Kang S, Lee H, et al. High efficiency and long lifetime of a fluorescent blue-light emitter made of a pyrene core and optimized side groups. ACS Appl Mater Interfaces 2018;10:30022.
[25] Parker CA, Hatchard CG. Delayed fluorescence from solutions of anthracene and phenanthrene. Proc R Soc (London) A Math Phys Sci 1962;269:574.
[26] Hochstrasser RM. The luminescence of organic molecular crystals. Rev Modern Phys 1962;34:531.
[27] Nieman CC, Robinson GW. Rapid triplet excitation migration in organic crystals. J Chem Phys 1962;37:2150.
[28] Kepler RG, Caris JC, Avakian P, et al. Triplet excitons and delayed fluorescence in anthracene crystals. Phys Rev Lett 1963;10:400.
[29] Kido JJ, Hayase H, Hongawa K, et al. Bright red light-emitting organic electroluminescent devices having a europium complex as an emitter. Appl Phys Lett 1994;65:24.
[30] Lamansky S, Kwong RC, Nugent M, et al. Molecularly doped polymer light emitting diodes utilizing phosphorescent Pt (II) and Ir (III) dopants. Org Electron 2001;2:53.
[31] Chen FC, Yang Y, Thompson ME, et al. High-performance polymer light-emitting diodes doped with a red phosphorescent iridium complex. Appl Phys Lett 2002;80:2308.
[32] Jin G, Liu JZ, Zou JH, et al. Appending triphenyltriazine to 1,10-phenanthroline: a robust electron-transport material for stable organic light-emitting diodes. Sci Bull 2018;63:446.
[33] Tanaka M, Noda H, Nakanotani H, et al. Effect of carrier balance on device degradation of organic light-emitting diodes based on thermally activated delayed fluorescence emitters. Adv Electron Mater 2019;5:1800708.
[34] Zhao L, Li C, Zhang Y, et al. Anthracene-cored dendrimer for solution-processible blue emitter: syntheses, characterizations, photoluminescence, and electroluminescence. Macromol Rapid Commun 2006;27:914.
[35] Zhao L, Zou JH, Huang J, et al. Asymmetrically 9,10-disubstituted anthracenes as soluble and stable blue electroluminescent molecular glasses. Org Electron 2008;9:649.
[36] Murgatroyd PN. Theory of space-charge-limited current enhanced by Frenkel effect. J Phys D 1970;3:151.
[37] Chiang CJ, Kimyonok A, Etherington MK, et al. Ultrahigh efficiency fluorescent single and bi-layer organic light emitting diodes: the key role of triplet fusion. Adv Funct Mater 2013;23:739.
[38] Ganzorig C, Fujihira M. A possible mechanism for enhanced electrofluorescence emission through triplet-triplet annihilation in organic electroluminescent devices. Appl Phys Lett 2002;81:3137.
[39] Sinha S, Monkman AP. Delayed electroluminescence via triplet-triplet annihilation in light emitting diodes based on poly[2-methoxy-5-(2′-ethylhexyloxy)-1,4-phenylene vinylene]. Appl Phys Lett 2003;82:4651.
[40] Rothe C, Monkman AP. Triplet exciton migration in a conjugated polyfluorene. Phys Rev B 2003;68:075208.
[41] Jankus V, Chiang CJ, Dias F, et al. Deep blue exciplex organic light-emitting diodes with enhanced efficiency: P-type or E-type triplet conversion to singlet excitons? Adv Mater 2013;25:1455.

Ling Peng is a Ph.D. student at the State Key Laboratory of Luminescent Materials and Devices, South China University of Technology (SCUT) under the guidance of Prof. Xu-Hui Zhu. Her work focuses on the design and synthesis of molecular blue emitters for organic light-emitting diodes.

Dongge Ma received his Ph.D. degree from Electrical Engineering Department of Jilin University in 1995. Then he worked successively as a visiting professor in Universidade Federal do Parana′l, Brazil, and a research fellow at Durham University and St. Andrews University, UK. He joined Changchun Institute of Applied Chemistry, Chinese Academy of Sciences, as a professor in 2001, and moved to South China University of Technology (SCUT) in 2016. His research interests are organic optoelectronic devices and physics, including OLEDs, OPDs and optoelectronic processes in organic semiconductors.

Xu-Hui Zhu received his Ph.D. degree at State Key Laboratory of Coordination Chemistry, Nanjing University in 2000. He then did postdoctoral work successively at Martin-Luther-Universät Halle-Wittenberg, Université d'Angers and Fudan University, and joined SCUT in 2004. His research interests include design and synthesis of organic π-electron systems with tailored properties for optoelectronics.